Science Journals

Central European Journal of Chemistry

Central European Science Journals CEJC 3(4) 2005 605-621

Oxygen detection using yttria-stabilized zirconia thin films doped with platinum

Dimitre Tz. Dimitrov*, Ceco D. Dushkin

Department of General and Inorganic Chemistry, Faculty of Chemistry, University of Sofia 1 James Bourchier Blvd., Sofia 1164, Bulgaria

Received 18 March 2005; accepted 24 May 2005

Abstract: Yttria stabilized zirconia (YSZ) thin films are obtained using both spray-pyrolysis and dip-coating. The ability of YSZ films incorporated with platinum nanospecies (Pt-YSZ) to detect oxygen is compared with that of pure YSZ thin films using a new experimental setup. With this system, the surface electrical resistance of the films as a function the oxygen content is measured at a fixed temperature. In addition, the effects of thermal annealing on the oxygen sensitivity of the films are observed. Platinum doped samples, Pt-YSZ, show different kinetics of carrier diffusion as compared to pure YSZ samples.

© Central European Science Journals. All rights reserved.

Keywords: Yttria stabilized zirconia (YSZ), YSZ thin films, platinum doped YSZ (Pt-YSZ), oxygen detection

1 Introduction

Yttria-stabilized zirconia (YSZ) is a widely studied and used material because of potential uses in important technological devices, such as solid oxide fuel cells, electrochemical solid-electrolyte oxygen sensors, ceramic oxygen generators, oxygen separation membranes, and membranes for the conversion of methane to syngas [1]. The working principle in all these devices is oxygen transport in the dense ceramic membranes [2]. One of the ways for a material to achieve higher values of ionic conductivity is to have a structure containing a large number of interconnected equivalent sites for mobile ions (Appendix A). These sites are only partially occupied if the zirconia crystal lattice is doped with yttrium [3]. In addition to doping with yttrium, the zirconia can be doped with other materials, or

^{*} E-mail: DTsenov@wmail.chem.uni-sofia.bg

other structure types can be used to improve the value of the ionic conductivity [1].

There should be different ways to vary the total conductivity of the material, which is important for its operation as an oxygen sensor. To achieve this goal we have added platinum (most likely in the form of a nanospecies), because it does not interact chemically with either the zirconium dioxide or the diffusing oxygen. One can assume that Pt will affect the ionic conductivity by changing both the vibration frequency of atoms and the crystal lattice condition.

There is little literature published relating the effect of metal (platinum) dopants on the behaviour of ceramic semiconductors. In reference [4], one of the major goals behind the design of a semiconductor-metal (TiO₂/gold) nanocomposite is the improvement of the catalytic properties or the tuning of the luminescence or sensing. The noble metal, which acts as a sink for photoinduced charge carriers, promotes the interfacial charge transfer process. The authors of [5] use Pt species to increase the capacitance per unit volume of YSZ capacitors. They discovered that the capacitance of electrolytically impregnated YSZ, sintered at 1200 °C, was enhanced by a factor of up to \sim 20 following the deposition of platinum at both electrodes. The most comprehensive study on the application of Pt in oxygen sensors is given in reference [6]. The authors describe an amperometric oxygen sensor containing a composite Pt-YSZ layer used as a diffusion barrier, facilitating the transportation and detection of oxygen. This layer is deposited on a bulk YSZ material with an overall thickness of 2-3 mm comprising pressed and sintered ceramic grains of a typical size of 1-1.5 μ m. The thickness of Pt-YSZ layer is between 1/12 and 1/2 the thickness of the YSZ layer. The platinum forms submicron particles with an average diameter of 0.1-0.6 μ m, depending upon the method of synthesis. Finer particles $(\sim 100 \text{ nm})$ are obtained using a sol-gel synthesis of the platinum powder. The fabricated sensor exhibits well-defined currents for oxygen concentrations up to 6 %, and the current response depends linearly on the concentration.

Unlike the cases of bulk powder-sintered ceramics [4-6], here we have utilized thin film coatings [7,8] of YSZ. The main advantage of using bulk ceramics YSZ in oxygen sensors [9] is the ability to obtain powders of high purity having uniform particle sizes which allows control of the sensor properties. However, when these samples are prepared using methods of thin film technology, the composition, structure and size of micro-crystallites depends intricately upon the technological conditions. Our observations are similar as discussed below.

Based upon the considerations addressed above, platinum is expected to influence the conductivity of YSZ thin films. For this purpose, we prepared YSZ films with and without Pt nanospecies using the methods of spray pyrolysis [7] and dip coating [8]. The surface resistance of samples was investigated using a home-built experimental setup. With this system, we measure the resistance of the thin films as a function of the oxygen content at a fixed temperature. A clear difference is observed between the behavior of samples with and without platinum nanospecies. In addition, the effects of the thermal annealing process on the oxygen sensitivity of the films are found. Platinum doped samples show different kinetics of carrier transport from those samples without doping.

2 Experimental methods

The YSZ thin films incorporated with platinum were prepared via the methods of spraypyrolysis [7] and dip-coating, using devices shown in [10] and [8], respectively, using an ethylene glycol solution of mixed metal citric complexes [11,12] as starting materials. For our investigation, we built the experimental setup shown on Fig. 1. It consists of a quartz container, in which the sample holder is placed. Two needle electrodes (thermoresistive wires with a diameter of 0.75 mm) were pressed into the upper part of the sample. We measured the surface resistance R, that can be defined as the ratio of DC voltage to the current flowing between two electrodes of specified configuration and that contact the same side of the film. The unit of surface resistance is the Ohm. Its value depends upon the distance between electrodes; therefore, the distance was kept constant at 8 mm throughout the measurements. The resistance of the sample was measured using digital voltmeter connected to the conductors coming from the sample. One of the conductors was thermoresistive wire passing through an aluminum flange via a dielectric tube; the other conductor was a steel stick holding the ceramic sample holder. This steel stick was connected to the aluminum flange, to which we connected the conductor for the measuring device. For measuring the resistance of samples in an oxygen-rich atmosphere, air was pumped into the system with an aquarium pump. For the oxygen free atmosphere, pure nitrogen was used. The quartz container with the sample was heated by a tube heater equipped with a regulated voltage source, which allowed for a gradual change in temperature. The temperature of the sample was measured using standard chromel-alumel thermocouple. The temperature was raised to about 1040-1090 K, and the temperature and the resistance of the sample were allowed to stabilize. The stabilization period was about 20 min. After stabilization, the sample was exposed to a nitrogen flow for about 20 min. After saturation, which was monitored by the sample resistance, the nitrogen flux was stopped, the system was allowed to equilibrate at that temperature. After 20 min at a constant resistance, the sample was exposed to air (with 21 % of oxygen). This procedure was repeated until the data were reproducible.

We tested two types of YSZ samples: with and without Pt nanospecies incorporated into the film. The deposition temperature for the spray pyrolysis was 525 K followed by annealing at 865 K for 2 hours. The films of about 30 μ m thickness were deposited onto a ceramic substrate, Rubalit R710 (for spray pyrolysis) or on R708 (for dip coating). The substrate size was 10×5 mm. The sprayed samples were of better quality than the dip coated samples (the latter having cracks originating during the deposition procedure). Samples contained zirconia ceramics doped with 15 mole % yttria for the pure YSZ sample and an additional 4 % Pt for the Pt-YSZ sample. Initially, the non-heated samples without Pt were white and transparent, whereas the samples with Pt looked greyish. After the thermal treatment during the measurement the samples with Pt became brown-black.

For simplicity, we assumed that the Pt doped samples contained metal nanospecies of platinum, although we did not study this point. This assumption was based on the synthetic method of the Pt doped YSZ. The procedure for doping the sol-gel for YSZ

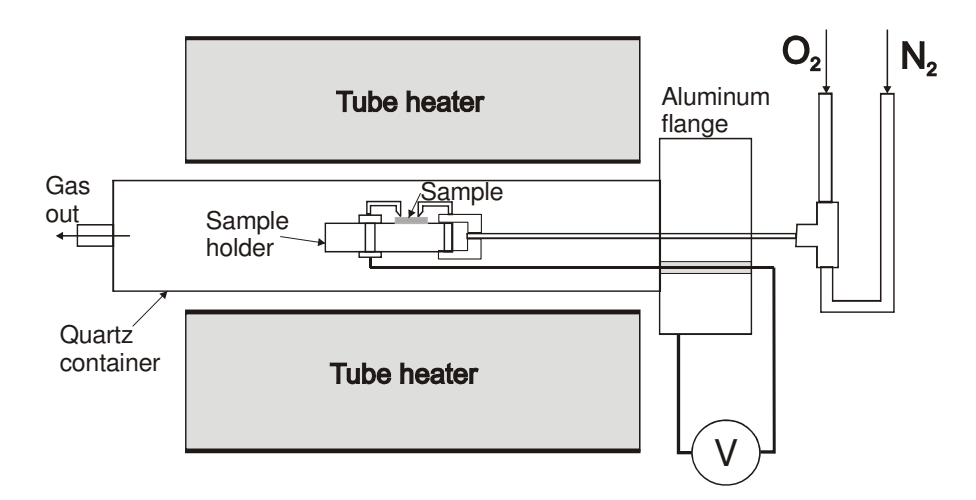


Fig. 1 Experimental setup for measuring the resistance of YSZ thin films at different oxygen contents (air with 21 % oxygen or pure nitrogen).

synthesis with Pt followed the literature preparation of platinum submicron- and nanoparticles [6]. More details for the preparation of YSZ and Pt-YSZ are given elsewhere [7].

During the experiment we varied the oxygen partial pressure by changing from blowing of air (using aquarium pump) to pure nitrogen. Both gases were dried by passing them through a flask with concentrated sulphuric acid. One experimental cycle consisted of blowing nitrogen until a steady resistance was reached, followed by exposure to air until a new steady condition of the resistance was obtained. Then the cycle was repeated. Two cycles on each sample were performed every day.

3 Result and discussion

3.1 Electrical behavior of YSZ and Pt-YSZ thin films under oxygen exposure

Figure 2 shows the dependence of the surface electrical resistance of the Pt-YSZ ceramics on the oxygen content. An increase in the sample resistance is always detected for the Pt doped samples at higher oxygen contents (21 % oxygen in air). During the first day, the resistance increases from 3.27 MOhm in a nitrogen atmosphere to 6.0 MOhm in the presence of oxygen. The signal reaches a maximum of 12 MOhm and then decays to a stationary value. Repeating the measurements gives similar patterns. The maximum change of the resistance occurs on the third day, increasing from 0.974 MOhm in a nitrogen atmosphere to 11.72 MOhm in air (during the second cycle). This noticeable increase in sensitivity towards oxygen with increasing of the annealing time could be due to a rearrangement of the crystal structure favoring the diffusion of oxygen in the YSZ thin film.

Adding Pt nanospecies to the sample probably leads to n-type conductivity – cf.

Fig. 8, below. In this situation, any increase in oxygen pressure lowers the electron concentration, which results in an enormous increase in the resistance as shown in Figure 2.

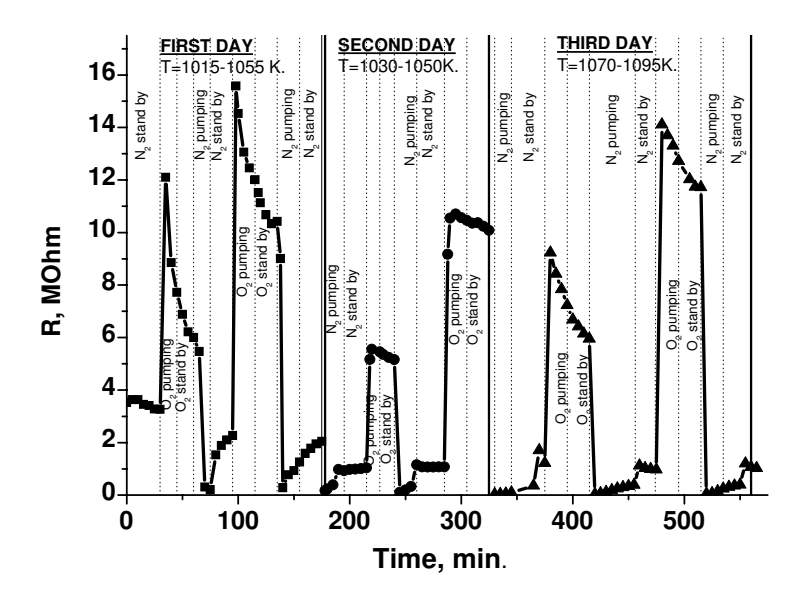


Fig. 2 Dependence of the surface resistance of Pt-YSZ thin films in an atmospheres of differing oxygen content. The sample is obtained by spray pyrolysis. The vertical solid lines separate the thermal treatment done during a particular day. The dotted vertical lines separate each cycle of thermal treatment. The time scale shows the total time of thermal treatment during all days. Shown also is the temperature of heating for each day. The time scale accounts for the total duration of thermal treatment.

For pure YSZ ceramics at atmospheric oxygen pressure, we expect p-type electroconductivity [3]. This is based upon the theoretical assumption with respect to the presence of impurities (in this case, yttrium atoms) having less charge than that of the zirconium cations in zirconium positions, leading to the formation of an equivalent number of oxygen vacancies. In contrast to the platinum doped YSZ, pure YSZ has no additional vacancies, because there is no change of the crystal lattice condition by the Pt nanoparticles. The lower number of vacancies are filled more easily with oxygen atoms as compared Pt doped YSZ, and we must take into account the oxygen concentration in the interstitial sites $\frac{1}{2}O_2 = O_i^x$, where O_2 is the oxygen in the gas phase. This situation is similar to the general case, in which oxygen in the interstitial sites is the main type of defect. In this case the total electroconductivity of the oxide depends upon the concentration of holes as $p \sim P_{O_2}^{1/4}$ (see Fig. 8 in Appendix A). Our measurements of pure YSZ obtained from spray pyrolysis and dip coating are shown in figures 3 and 4, respectively. As seen in figure 3, oxygen exposure results in a reduced resistance from 1.25 MOhm to 0.75 MOhm of the sample obtained by spray pyrolysis during the first 150 min of measurement. During this time, the concentration of oxygen is increasing in the interstitial sites. This oxygen is further ionized by the routes $O_i^x = O_i^- + p^+$ and $O_i^- = O_i^{2-} + p^+$ where p^+ is a hole. This increases the number of holes and lowers the resistance of the sample.

We observed almost the same features for pure YSZ films obtained by dip coating. In this case, we found a reduction of the sample resistance from 1.1 MOhm to 0.6 MOhm

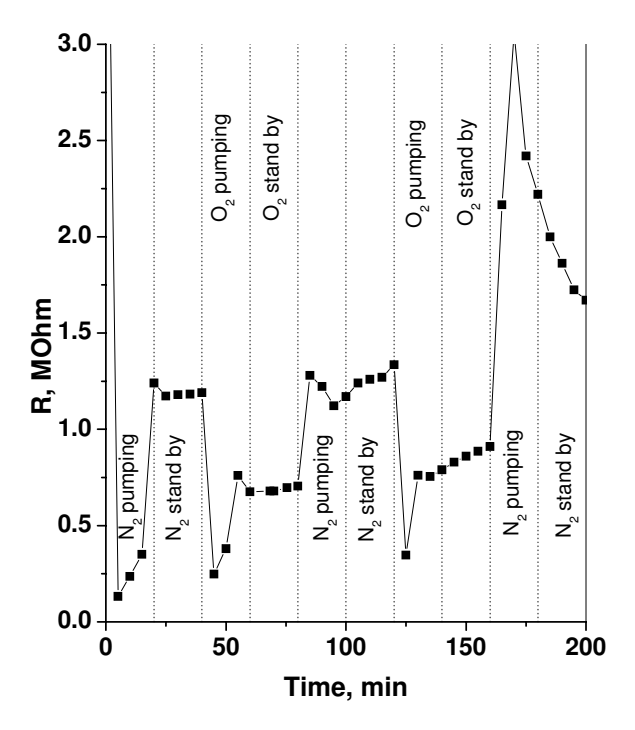


Fig. 3 Dependence of the resistance of pure YSZ in an atmosphere of differing oxygen content at 1060 K, measured during the first day of the experiment. The sample is obtained by spray pyrolysis. The data show a transition from low (1st and 2nd cycle) to high resistance under nitrogen atmosphere (3rd cycle).

after exposure to oxygen as compared to pure nitrogen – Fig. 4.

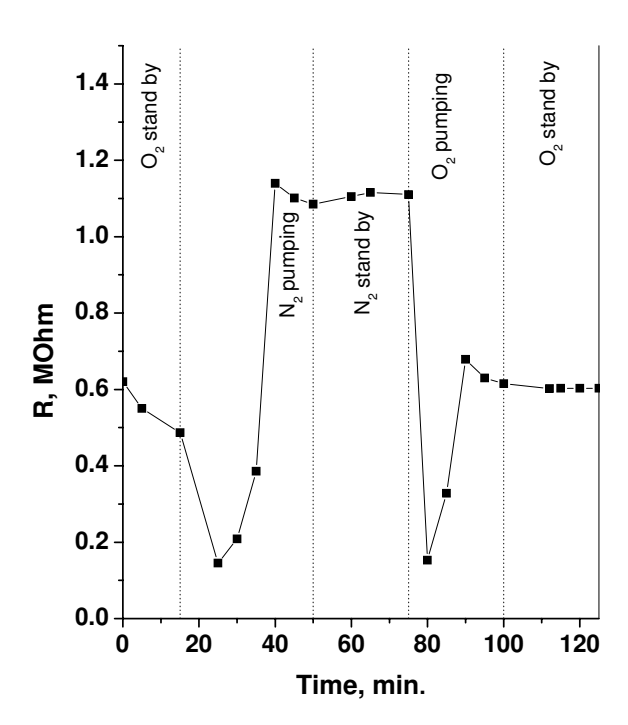


Fig. 4 Dependence of the resistance of pure YSZ in an atmosphere of differing oxygen content at 1062-1085 K, third day. The sample is obtained by dip coating.

As stated in Appendix A, when the oxygen vacancy concentration is determined by

the yttrium cations [3], both the diffusion coefficient, D_r , and the ionic conductivity of the material determined by the potential energy of the non-elastically deformed crystal lattice U_{ZrO_2} via the migration enthalpy ΔH_m . For higher values of conductivity, many vacancies, free from oxygen atoms, would be obtained. The number of electrons will decrease with the oxygen pressure, similar to the general case, in which the concentration of the electrons changes with the oxygen pressure P_{O_2} as $n \sim P_{O_2}^{-1/4}$ – see Fig. 8 in Appendix A. This will decrease the conductivity of the sample. As can be seen from equation (A2), one of the ways to obtain higher value of the oxygen diffusion coefficient is to reduce the value of ΔH_m , which could be changed by both the vibration frequency of atoms ν and the crystal lattice condition. Using a Born-Haber cycle [3,13] for our system (Appendix B), the energy of crystal lattice U_{ZrO_2} is affected by the heat capacity of the material, which is greatly influenced by the vibration frequency of atoms ν (Appendix C).

When the distances between the atoms increase [14], they vibrate at lower frequencies, and higher amplitudes for the same value of energy. Hence, by introducing species that do not interact chemically with both zirconium dioxide and diffused oxygen mostly affects the vibrational frequency of the atoms. This, in turn, influences the potential energy of the non-elastically deformed crystal lattice and has an impact on the diffusion coefficient of oxygen and, consequently, on the ionic conductivity of that material. In addition to vacancies formed by the yttrium cations, the number of vacancies will increase due to the crystal lattice deformed by platinum nanospecies.

3.2 Effects of the thermal annealing process on the oxygen sensitivity of the films

Because there are no data available using YSZ thin films, reinforced with platinum nanospecies, as oxygen sensors, we cannot comment on the durability of this structure (see reference [6] for the stability of Pt-YSZ bulk ceramics sensors). As can be seen in figure 2, the resistance of the Pt-YSZ thin film is relatively stable with time. In a nitrogen atmosphere, the resistance of the sample decreases from an initial value of 3.27 MOhm at the beginning of the first day to a value 1.05 MOhm at the end of the third day. The final resistance in the oxygen atmosphere gradually increases from 6.15 MOhm at the first cycle on the first day to 11.75 MOhm at the second cycle on the third day. These changes for the three days run occur over a total of 560 min. The reduced sample resistance is probably due to an increase in the number of oxygen vacancies beyond those formed by both yttrium doping and the Pt nanospecies. It is reasonable that this will increase the effect of oxygen on the sample resistance as noticed above. However, further annealing processes lead to reverse change in the electrical behavior of the sample. As shown in figure 5, a gradually reduced resistance is observed upon exposure to oxygen (and a gradual increase of the resistance in nitrogen atmosphere). This could be due to the destruction of some of the platinum nanoparticles, transforming the conductivity of the sample from n-type into p-type. In this case the behavior is similar to the behavior of undoped samples shown in Fig. 3 and Fig. 4 above.

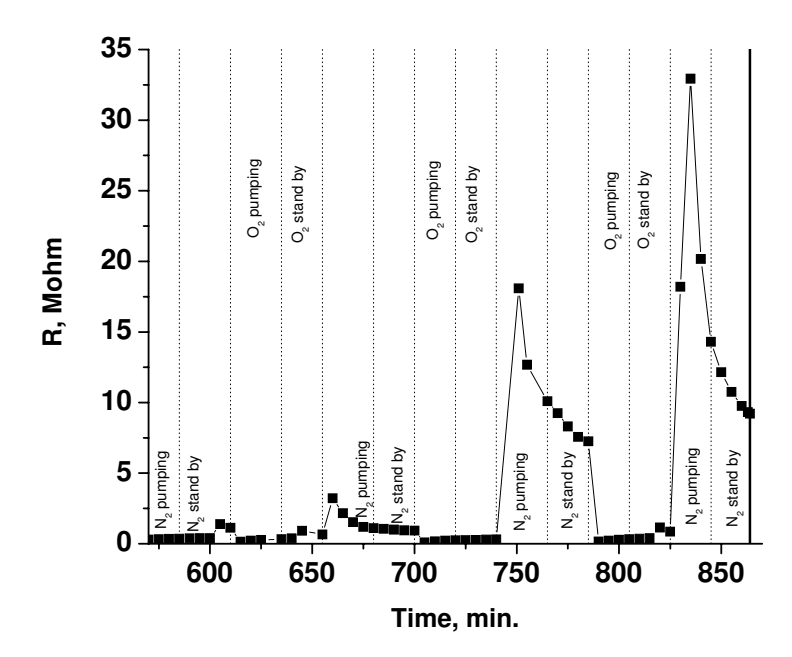


Fig. 5 Dependence of the surface resistance of Pt-YSZ sample in an atmosphere of differing oxygen content (fourth day). The sample is the same as that whose resistance is shown in Fig. 2 for 550 min. The temperature of measurement is further increased, because at a temperature 1065-1075 K, there is no effect of the gas change on the resistance. Shown is the transition from increased resistance to decreased resistance in oxygen.

In the case of the pure YSZ samples produced by dip-coating, the resistance changes during all three days runs. But the oxygen exposure always leads to a reduction of the resistance consistent with the model of increasing conductivity of the sample due to an increase in the concentration of holes. Such a behavior is observed after 150 min in figure 3 for pure YSZ samples produced by spray pyrolysis. However, during the second day run, a gradual increase of the resistance upon oxygen exposure is observed, eventually producing an enormous increase in the resistance in an oxygen atmosphere (Fig. 6). This change in electrical behavior for the undoped sample requires future explanation. It is not surprising, however, as the properties of thin film ceramics depend upon a complexity of technological conditions [9]. We can assume that some distortions of the yttrium stabilization of the zirconia leads to a structure in which n-type conductivity is more favorable. If so, increasing the oxygen concentration will change the sample conductivity to inherent conductivity, because the oxygen vacancies are blocked by diffused oxygen atoms.

The sample of pure YSZ obtained by spray-pyrolysis is stable for only 150 min. This is much lower as compared to 550 min for the sample with Pt nanoparticles obtained by the same method.

3.3 Dynamics of the charge carriers

The transition curves for the resistance in the above figures show a time dependence R(t). It is a measure of the relaxation of the charge carriers in the ceramic film toward the

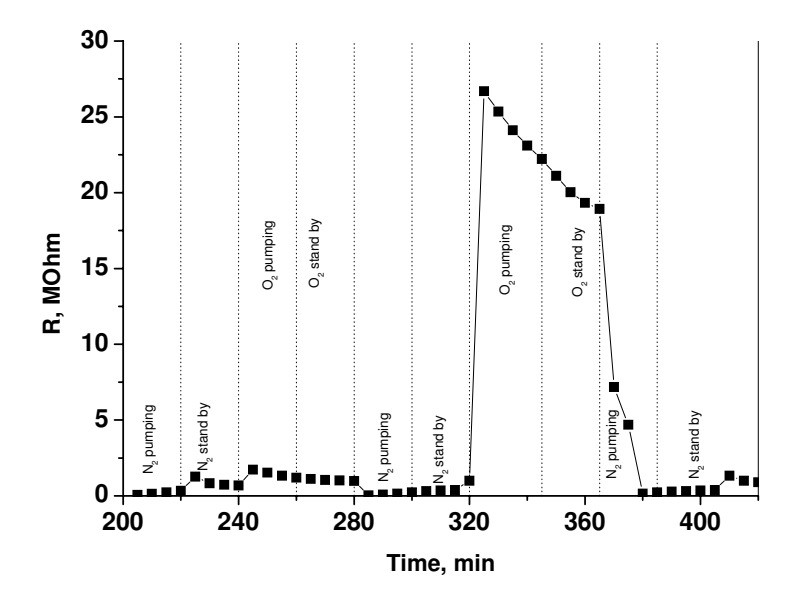


Fig. 6 YSZ Dependence of the resistance of pure YSZ in an atmosphere of different oxygen concentrations at 1090 K measured during the second day of the experiment. The sample is obtained by spray pyrolysis and is the same as that in Fig. 3.

equilibrium value, R_{eq} , under certain conditions. In Fig. 7, we compare three transition curves for representative runs. The fastest relaxation occurs for the sample with Pt nanoparticles during the first heat treatment. The slowest relaxation occurs for the sample of pure YSZ. This means that the presence of metal nanospecies enhances the motion of charge carriers. After three runs of thermal treatment, however, the relaxation of the sample with nanoparticles becomes slower, which implies that there are irreversible changes occurring in the sample.

4 Conclusions

Here we compare the electrical behavior of two types of thin films of yttria stabilized zirconia (YSZ): (i) films of pure YSZ; and (ii) films of Pt-YSZ, which contain platinum nanospecies. These films are prepared by either spray pyrolysis of the material on a heated substrate or dip coating of a substrate at ambient temperature. The electric resistance of the samples is measured using a specially constructed setup comprised of a quartz container with metal flange for housing the sample in an atmosphere of varying oxygen content. Ambient air provides high oxygen content, and pure nitrogen creates environment of no oxygen. Alternating the supply of oxygen and nitrogen changes the sample resistance depending upon the prevailing type of electroconductivity. During the first 150 min of thermal treatment, the pure YSZ films have a higher resistance (low conductivity) in nitrogen (zero oxygen) and have lower resistance (higher conductivity) in oxygen (21 % in air). The prevailing conductivity type occurs via the holes created due to the ionization of oxygen atoms in the interstitial sites. In contrast, the Pt-YSZ films have a higher resistance when oxygen is flowing in the container and have a lower

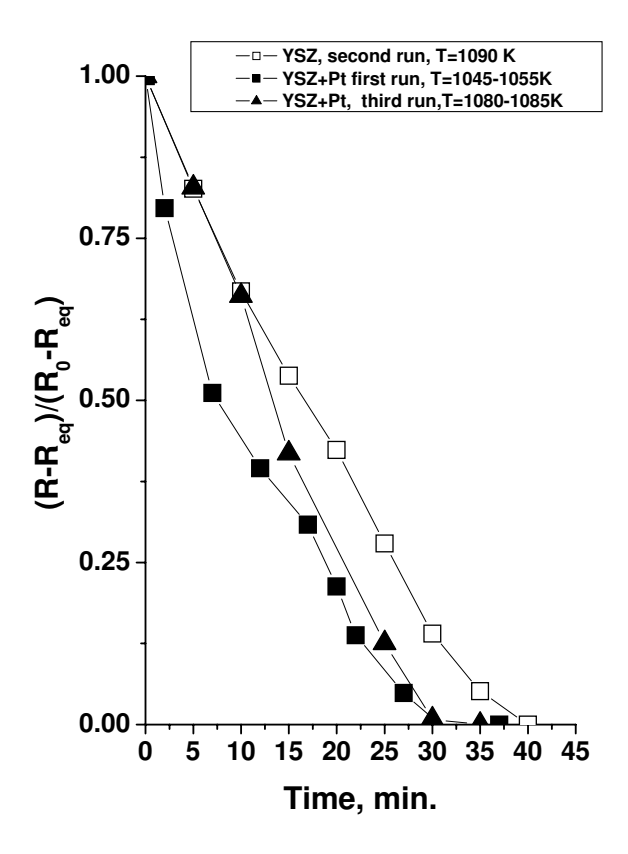


Fig. 7 Normalized kinetic dependence of the resistance of YSZ and Pt-YSZ samples in an oxygen atmosphere. The samples are obtained by spray pyrolysis. R_0 is the initial surface resistance; R_{eq} is the equilibrium resistance at the end of relaxation.

resistance in the absence of oxygen during the first 550 min of treatment. Increasing the oxygen content decreases the number of electrons in the film lowering the conductivity (increasing the resistance). Probably, the role of the platinum nanospecies is to disturb the YSZ crystal lattice, which affects both the diffusion of oxygen and the ionic conductivity of the material. The changes of the resistance from oxygen exposure to nitrogen exposure of the Pt-YSZ sample are much higher compared of that of the pure YSZ sample. It is also clear that the Pt-YSZ sample is stable for a much longer period of time than the pure YSZ sample.

Regarding the transient conductivity of the Pt-YSZ samples, the charge carriers relax faster toward the equilibrium state than the pure YSZ samples.

In conclusion, future investigation is required to quantitatively prove the observed effect of the platinum nanoparticles on the conductivity under oxygen exposure as compared to that of pure YSZ films. These future studies will determine the possibility of their application as oxygen sensors.

Acknowledgment

The financial support of grant X-1210 from the Bulgarian Ministry of Education and Science is greatly acknowledged. The authors thank Dr. Dimiter Todorovsky (Chemistry

Faculty) for his support and valuable comments on the research. The authors are also grateful to Mr. Kaloian Kaloianov (Physics Faculty) and Mr. Antony Abadjimarinov (Institute of Physical Chemistry, Bulgarian Academy of Sciences) for their master work on the experimental setup.

References

- [1] S.J. Skinner and J.A. Kilner: "Oxygen ion conductors", *Materialstoday*, Vol. 3, (2003), pp. 30–37.
- [2] J.A. Kilner: "Fast oxygen transport in acceptor doped oxides", *Solid State Ionics*, Vol. 129, (2000), pp. 3–23.
- [3] P. Kofstad: Nonstoichiometry, Diffusion and Electrical Conductivity in Binary Metal Oxides, Wiley-Interscience, New York, 1972.
- [4] A. Dawson and P.V. Kamat: "Semiconductor-metal nanocomposites. Photoinduced fusion and photocatalysis of Gold-Capped TiO₂ (TiO₂/gold) nanoparticles", *J. Phys. Chem. B*, Vol. 105, (2001), pp. 960–966.
- [5] M.G.H.M. Hendriks, B.A. Boukamp, J.E. ten Elshof, W.E. van Zyl and H. Verweij: "The electrical behaviour of platinum impregnated porous YSZ", *Solid State Ionics*, Vol. 146, (2002), pp. 123–132.
- [6] Z. Peng, M. Liu and Ed. Balko: "A new type of amperometric oxygen sensor based on a mixed-conducting composite membrane", *Sensor Actuators B*, Vol. 72, (2001), pp. 35–40.
- [7] R. Todorovska, N. Petrova and D. Todorovsky: "Spray pyrolysis deposition of YSZ and YSZ-Pt composite films", *Appl. Surface Sci.*, submitted.
- [8] C. Dushkin, S. Stoianov, A. Bojinova and S. Russev: "Dip coating apparatus for deposition of TiO₂ films", Ann. Univ. Sofia Fac. Chim., submitted.
- [9] A.I. Buturlin, T.A. Gabyzian, N.A. Golovanov, I.V. Baranenkov, A.V. Evdokimov, M.N. Murshudli, V.G. Fadin and Yu.D. Shistiakov: "Gas sensitive sensors based on metal oxides semiconductors", *Rev. Foreign Electronic Ind.*, Vol. 10, (1983), pp. 3–39 (Journal of the Ministry of Electronic Industry of USSR, in Russian).
- [10] R.V. Todorovska, St. Grodeva-Zotova and D.S. Todorovsky: "Spray pyrolysis deposition of α Fe₂O₃ thin films using iron (III) citric complexes", *Mater. Lett.*, Vol. 56, (2002), pp. 770–774.
- [11] N. Petrova, R. Todorovska, D. Todorovsky and D. Shopova: "Yttrium-zirconium citric complexes as starting material for preparation of YSZ powders and layers", *Key Eng. Mater.*, Vol. 264–268, (2004), pp. 427–430.
- [12] N. Petrova and D. Todorovsky: "Thermal decomposition of zirconium-yttrium citric complexesprepared in ethylene glycol and water media", *Mater. Res. Bull.*, submitted.
- [13] F.A. Kroöger: The Chemistry of Imperfect Crystals, North-Holland Publ. Co., Amsteram, 1964.
- [14] L.D. Landau and E.M. Lifshitz: *Theoretical Physics*, Vol. 5, In: *Statistical Physics*, part 1, Nauka-Physmathlitr, Moscow, 1995 (in Russian).
- [15] B.F. Ormont: An introduction in chemical physics and crystal chemistry of semiconductors, Visshaya Shkola, Moscow, 1973 (in Russian).

Appendix A

Theoretical background of the detection of oxygen using YSZ ceramics

An inspection of the ionic conductivity equation [2]

$$\sigma = NN_A \frac{q^2}{R_G T} \gamma [V_O^{2+}]_S (1 - [V_O^{2+}]_S) a_0^2 \nu_0 \exp\left(-\frac{\Delta H_m}{R_G T}\right)$$
(A1)

reveals that the migration enthalpy, ΔH_m , is one important factor in the determination of the ionic conductivity, σ . The other quantities in equation (A1) are as follows: $[V_Q^{2+}]_S$ is the concentration of the doubly ionized oxygen vacancies, (expressed as a site fraction); a_0 is the crystal lattice parameter; ν_0 is the characteristic lattice frequency at equilibrium; N is the volume concentration of mobile ions; N_A is the Avogadro number; q is the vacancy charge; sites, f is the correlation factor, ΔS_m is the entropy of migration [2]; T is the absolute temperature; and R_G is the universal gas constant. Some of the quantities included in the above equation are constants, while the others, N, γ , a_0 and ν_0 , are not expected to vary substantially from oxide to oxide [2]. The value of ΔH_m is determined by the potential energy of the non-elastically deformed crystal lattice, U_{ZrO_2} [3]. If it were possible to increase the distance between the atoms, which would lower the vibration frequency of the atoms, the YSZ crystal lattice would be deformed as well. Because of that we also expect a change in the conductivity from hole-type (p-type) to electron-type (n-type). The possibility of obtaining the different conductivities (n- or p-type) depends upon the ability of oxygen to leave regular oxygen positions forming oxygen vacancies or diffusing into interstitial sites, which is determined by the crystal lattice condition.

When the oxygen vacancy concentration is determined by the yttrium cations, [3]:

$$D_r = \alpha a_0^2 \nu_0 [Y_{Zr}^{1-}] \exp\left(\frac{\Delta S_m}{R_G}\right) \exp\left(-\frac{\Delta H_m}{R_G^T}\right)$$
 (A2)

where D_r is the diffusion coefficient along the vacancies; α is a geometrical factor; $[Y_{Zr}^{1-}]$ is the concentration of yttrium ions in zirconium positions having a negative effective charge.

The variation of conductivity as a function of the oxygen concentration is important for the application of YSZ thin films as oxygen sensors. The dependence of the conductivity on both the temperature and the oxygen pressure is analyzed in reference [3] for the general case of oxides with the number of oxygen vacancies determined by the number of low charged impurity cations situated in the oxygen positions of the zirconia crystal lattice. For high oxygen pressures, the ionic conductivity does not depend on the oxygen pressure. When the concentration of impurity (yttrium) determines the concentration of oxygen vacancies, then $V_O^{2+} > n + p$ (n is the concentration of electrons, p is the concentration of holes). In this case, the total electroconductivity of the oxide depends upon the relationship between V_O^{2+} and n+p, which depends in turn on the oxygen pressure $(n \sim P_{O_2}^{-1/4}$ for electrons and $p \sim P_{O_2}^{1/4}$ for holes). Consequently, the conductivity of the

oxide could be ionic, electronic, or of mixed type. The temperature dependence of the ionic conductivity coincides with the temperature dependence of the diffusion coefficient of the main ionic carriers [3]. Dependent upon the relationship $V_O^{2+}/(n+p)$, oxides having a low charged impurity could be p- or n-type semiconductors [3].

Let us consider the crystalline lattice of zirconia, ZrO_2 , doped with yttria, Y_2O_3 , with the general formula $Zr_{1-x}Y_xO_{2-\delta}$, where δ is the deviation from stoichiometry [1]. The lattice is of fluorite type. The presence of yttria creates defects in the zirconia sublattice. The presence of impurities having a charge less than the charge of zirconium cations in a zirconium position leads to the formation of equivalent number of oxygen vacancies [3]. For each yttrium atom, two oxygen vacancies will be formed according to the equation:

$$Y_Y^{3+} + Zr_{Zr}^{4+} + 2O_O = Y_{Zr}^{1-} + 2V_O^{2+} + Zr_i^{4+} + 4e^- + O_2$$
 (A3)

Here Y_Y^{3+} means yttrium ion in a regular position into the Y_2O_3 lattice; Zr_{Zr}^{4+} means zirconium ion in a regular position into the ZrO_2 lattice; O_O means oxygen atom in a regular oxygen position; Y_{Zr}^{1-} means yttrium ion in zirconium position of effective charge -1; V_O^{2+} means a double ionized oxygen vacancy obtained following the route $V_O^x = V_O^{1+} + e^-$ and $V_O^{1+} = V_O^{2+} + e^-$, where V_O^x means a neutral oxygen vacancy and V_O^{1+} means a single ionized oxygen vacancy; Zr_i^{4+} means zirconium ion in interstitial sites in the ZrO_2 lattice. A neutral oxygen vacancy is created by the equation $O_O = V_O^x + \frac{1}{2}O_2$ where oxygen is transported from the sublattice of oxygen in ZrO_2 to the gas phase.

To avoid complication in equation (A3), the equation of oxygen vacancy formation could be written, following the route of [3], as

$$O_O = V_O^{2+} + 2e^- + \frac{1}{2}O_2$$
 (A4)

The electronegativity equation gives

$$2[V_O^{2+}] = [Y_{Zr}^{1+}] + n \tag{A5}$$

where n is the electron concentration. In the case of equilibrium of the point defects can be expressed as

$$[V_O^{2+}]n^2 P_{O_2}^{1/2} = K_{V_O^{2+}} \tag{A6}$$

where $K_{V_O^{2+}}$ is the equilibrium constant of formation of the doubly ionized oxygen vacancies.

Equation (A5) has two limiting cases:

(i) The number of electrons created by the ionization of neutral oxygen vacancies is much greater than the number of yttrium cations in Zr positions, i.e. $n = 2[V_O^{2+}] \gg [Y_{Zr}^{1-}]$. In this case the number of impurities (yttrium cations) does not affect the equilibrium concentration of the native point defects. Therefore, the concentration of electrons and oxygen vacancies can be determined by the following equation:

$$\frac{1}{2}n = [V_O^{2+}] = \left(\frac{1}{4}K_{V_O^{2+}}\right)^{1/3}P_{O_2}^{-1/6} \tag{A7}$$

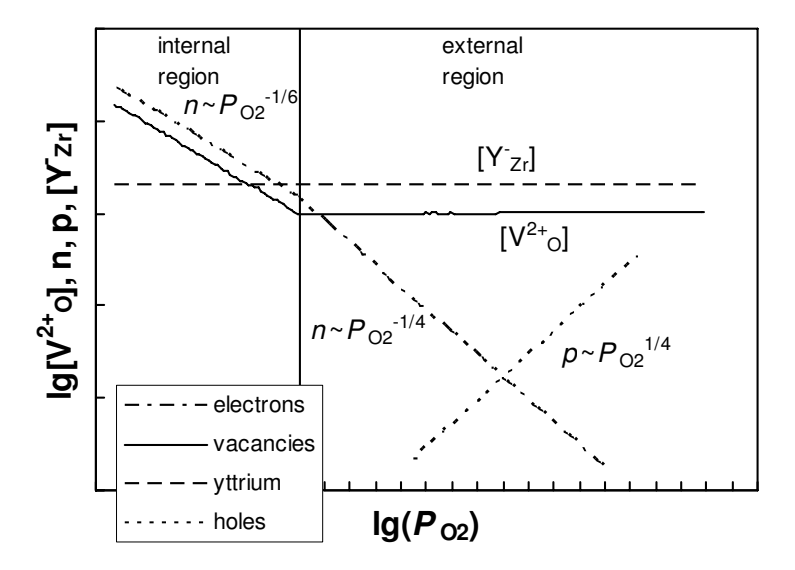


Fig. 8 Schematic dependence of the concentrations of electrons, vacancies, yttrium cations, and holes on the oxygen pressure in YSZ [3].

This situation can be observed at low oxygen pressure, hence, at a high oxygen deficiency – the internal region of figure 8.

(ii) The number of oxygen vacancies is determined by the impurity (yttrium cations) at the limit, $[Y_{Zr}^{1-}] = 2[V_O^{2+}] \gg n$. This is the external region in Fig. 8. Therefore, the electron concentration can be determined as

$$n = \frac{\left(K_{V_O^{2+}}\right)^{1/2}}{\left[Y_{Z_T}^{1-}\right]} P_{O_2}^{-1/4} \tag{A8}$$

In this situation, any increase of the oxygen pressure will reduce the concentration of electrons, which results in an enormous increase of the resistance. This is observed for the initial measurement of Pt-YSZ in Fig. 2.

At higher oxygen concentration, we must take the ionization of holes into account. The inherent conductivity will be given as $np = K_i$, where K_i is the inherent equilibrium constant. For writing the electronegavity equation, we must take the concentration of holes into account, $2[V_O^{2+}] + p = n + [Y_{Zr}^{1-}]$. Hence, the concentration of holes will change proportionally to the partial pressure of oxygen according to the equation

$$p = \frac{K_i[Y_{Zr}^{1-}]}{2\left(K_{V_O^{2+}}\right)^{1/2}} P_{O_2}^{1/4} \tag{A9}$$

The concentration of holes is determined by the concentration of oxygen in the interstitial sites $O_i^x = \frac{1}{2}O_2$, where O_2 is the oxygen in the gas phase. This oxygen is further ionized by the routes $O_i^x = O_i^- + p^+$ and $O_i^- = O_i^{2-} + p^+$, where p^+ is a hole.

Figure 8 shows that when yttria is added to zirconia the conductivity can be p- or n-type depending on the oxygen pressure. Increasing the concentration of holes decreases the sample resistance in samples without Pt. That is why YSZ can be used as a solid

phase electrolyte for oxygen detection. In such a system, one observes ionic conductivity over a broad range of oxygen pressures.

Appendix B

Born-Haber cycle for the YSZ ceramics

In the Born-Haber cycle, the heat of formation of one ionic compound, ΔH_{ZrO_2} , is expressed by the energy of crystal lattice, U_{ZrO_2} , the ionic potential of zirconium, I_{Zr} , the electron affinity of oxygen, A_O , the enthalpy of sublimation, $\Delta H_{Zr,subl}$, and the dissociation energy of oxygen, E_{O_2} [3,13]. For the formation of zirconium dioxide from a solid metal and diatomic oxygen, this cycle is expressed by the following reactions:

$$Zr ext{(solid)} = Zr ext{(gas)} + \Delta H_{Zr,subl}$$

$$Zr(gas) = Zr^{4+}(gas) + 4e^{-} + \sum 4I_{Zr}$$

$$O_{2}(gas) = 2O(gas) + E_{O_{2}}$$

$$2O(gas) + 4e^{-} = 2O^{2-}(gas) + \sum 4A_{O}$$

$$Zr^{4+}(gas) + 2O^{2-}(gas) = ZrO_{2}(solid) - U_{ZrO_{2}}$$

Total reaction: $Zr(solid) + O_2(gas) = ZrO_2(solid) + \Delta H_{ZrO_2}$.

The enthalpy of formation ΔH_{ZrO_2} is derived from this circular process:

$$\Delta H_{ZrO_2} = \Delta H_{Zr,subl} + \sum 4I_{Zr} + E_{O_2} + \sum 4A_O - U_{ZrO_2}.$$
 (B1)

Appendix C

Effect of the distance between the atoms on the YSZ properties

When the distance between the atoms increases, they vibrate at lower frequencies and higher amplitudes (for the same value of energy) [14]. Therefore, introducing nanoparticles that do not interact chemically with either the zirconium dioxide or the diffused oxygen, the frequency of vibrations of the atoms is reduced. Decreasing of the frequency affects the characteristic temperature of the zirconium dioxide, $\Theta = \beta \nu = h\nu/k$, where ν is the frequency of vibration of the atoms, μ is Planck's constant, and μ is the Boltzman constant, μ is the Lindeman formula, μ is the vibrational frequency of the atoms can be calculated using the Lindeman formula, $\nu = 2.8 \times 10^{12} \sqrt{\frac{T_s}{AV^2/3}}$, where T_s is the melting temperature, T_s is the atomic weight, and T_s is the atomic volume. The expression for T_s is given as T_s is the atomic weight, and T_s is the high temperature region (from 30 K to 300 K and more) we can use the Nernst-Lindeman's formula [15]:

$$c_v = \frac{3}{2} R_G \left[\frac{e^{\frac{\Theta}{T}} \left(\frac{\Theta}{T} \right)^2}{\left(e^{\frac{\Theta}{T}} - 1 \right)^2} + \frac{e^{\frac{\Theta}{2T}} \left(\frac{\Theta}{2T} \right)^2}{\left(e^{\frac{\Theta}{2T}} - 1 \right)^2} \right]$$
(C1)

The value of the heat capacity at constant pressure, c_p , is found by using the expression $c_p = c_v + 0.0214c_v^2 \ T/T_S$. Applying Kirchoff's law, ΔH_{ZrO_2} is found at a given temperature. An initial reaction temperature of 0 K produces the following equation:

$$\Delta H_T = \Delta H_0 + \int_0^T \Delta \sum c_p \ dT.$$